

CHARACTERIZATION OF SLIP LINES IN SINGLE EDGE NOTCHED TENSION SPECIMENS

F. Van Gerven¹, W. De Waele¹, D. Belato Rosado¹ and S. Hertelé¹

¹ Ghent University, Soete Laboratory, Belgium

Abstract: The application of slip line analysis in weld failure assessment has not gained much attention to date. The presented research aims to predict slip line patterns taking into account the complex heterogeneous structure of the weld. A preliminary study based on Single Edge Notched Tension (SENT) test results sampling pure base material, i.e. not containing any welds is conducted to assess the impact of side grooves on slip line behaviour and to validate slip line theory and finite element analysis.

Keywords: SENT, slip line, side grooves, digital image correlation

1 INTRODUCTION

Soete Laboratory's ongoing research in improving engineering critical assessments (ECA) of flawed welds aims at implementing local weld heterogeneity patterns into the flaw assessment. The importance of ECA is illustrated in reference [1], which mentions a pipeline project for which around 2% overall project savings could be achieved from the application of ECA. Having a model that takes into account weld heterogeneity could improve the accuracy of ECAs and thus save the industry a considerable budget, improve safety and reliability. Reliability is related to the limit states that are considered. Assessing the uncertainty on each ECA parameter rather than using bounding theorems reduces conservatism, accumulation of uncertainty effects and hence promotes overall safety [1]. In light of obtaining such heterogeneity models, the theory of slip lines is used by Soete Laboratory as a starting point.

Slip lines represent the paths of maximum shear stress, originating at the crack tip, upon the application of a primary load. In the framework that accounts for effects of weld metal heterogeneity, it is assumed that the material properties along these slip lines govern the crack driving force implied by the load. Therefore, knowledge of slip line patterns is essential to the sound application of the framework.

This paper focuses on the experimental and numerical identification of slip line patterns in Single Edge Notched Tension (SENT) specimens. The SENT test has recently gained interest in research areas where crack tip loading is characterized by a low level of crack tip constraint (e.g. defects in pipeline girth welds). The results of this study thus provide a validation basis for applications of slip line theory in non-homogeneous structures.

The paper is structured as follows. Section 2 gives an introduction into the slip line theory from which a theoretical solution for the given problem can be extracted. In section 3 an introduction into SENT testing is given, while sections 4 and 5 give details about the experimental and numerical procedures followed. Section 6 presents the results with their appropriate discussion, and section 7 finally concludes.

2 SLIP LINE THEORY

Slip line theory, as reported by Hill [2], Gao [3] and Johnson [4] starts from some assumptions to enable an analytical solution.

1. A rigid – perfectly plastic solid, i.e. having an infinite yield Young's modulus and no work hardening upon plastic deformation
2. Plane strain deformation in the (x,y) plane, i.e. $\sigma_{zz} = \frac{1}{2}(\sigma_{xx} + \sigma_{yy})$ and $\varepsilon_{zz} = 0$
3. Quasi-static loading
4. No temperature changes and no body forces
5. Isotropic material
6. No Bauschinger effect

Under these assumptions, the equilibrium equations and yield criterion result in three equations for the three unknown stress components in plane strain deformation $\sigma_{xx}, \sigma_{yy}, \sigma_{xy}$. The solution that is postulated, satisfies the equations above and gives rise to a set of hyperbolic equations resulting in a set of characteristics, referred to as the Hencky relations. Hereby, the critical shear stress k is assigned $\sigma_{YS}/2$ or

$\sigma_{YS}/\sqrt{3}$ depending on the use of von Mises' or Tresca's yield criterion and p represents the hydrostatic pressure.

$$\sigma_{xx} = -p - k \sin 2\varphi \quad (1)$$

$$\sigma_{yy} = -p + k \sin 2\varphi \quad (2)$$

$$\tau_{xy} = k \cos 2\varphi \quad (3)$$

$$\sigma_{zz} = -p \quad (4)$$

The two families of characteristics α and β , named slip lines, are perpendicular to each other, with the convention that α lines have an angle φ with respect to the x -axis.

$$p + 2k\varphi = \text{constant on an } \alpha \text{ - line} \quad (5)$$

$$p - 2k\varphi = \text{constant on an } \beta \text{ - line} \quad (6)$$

A similar argumentation can be conducted for the velocity components. The plane strain assumption results in a zero z -velocity, and non-zero x - and y -velocities v_x and v_y . Starting with the continuity and isotropy equations, a set of two velocity characteristic families can be deduced, having the same directions as the stress characteristics. From this, the following set of equations is derived, with u the velocity in the α direction and v in the β direction.

$$du - v d\varphi = 0 \quad \text{on an } \alpha \text{ - line} \quad (7)$$

$$dv + u d\varphi = 0 \quad \text{on a } \beta \text{ - line} \quad (8)$$

This set of equations is also referred to as the Geiringer equations. Furthermore, the coinciding characteristics of stresses and velocities indicate that the direction of maximum shear stress and shear strain-rate are equal.

Generally, both stress and velocity boundary conditions are needed to obtain a solution for the slip line field. One boundary condition of major importance is the stress free surface boundary, meaning that no normal and shear stress component can exist at the surface. Consequently, the normal and tangential direction at the free surface are directions of principle stress. As slip lines are lines of maximal shear stress in the material, they consequently intersect the free surface at an angle of $\pm 45^\circ$ [2].

3 SENT TESTING

This paper aims at validating post-processing tools in the determination of slip line patterns. Single Edge Notch Tension (SENT) tests are to this purpose performed experimentally on a test rig and numerically in the commercial finite element software ABAQUS[®]. Both have proven their accuracy in previous papers published by Soete Laboratory [5]–[8]. SENT test specimens, schematically shown in figure 1, have a rectangular cross section with a pre-machined notch a_0 and are subjected to a tensile load. The exact boundary condition can vary, and here the specimen is clamped. In order to extend the experimental and numerical evaluation to slip line identification, postprocessing routines have been developed using Matlab[®] and Python[™]. By performing the experiment and numerical simulation for a grooved and non-grooved specimen, the effect of side grooves in SENT tests on the slip line pattern at the specimen surface can be determined. Side grooves are applied in order to create a certain level of triaxiality at the specimen surface, just as is the case at the specimen mid-width. The latter encourages the crack to grow uniformly throughout the specimen width [9], [10], although the influence on slip lines is unsure.

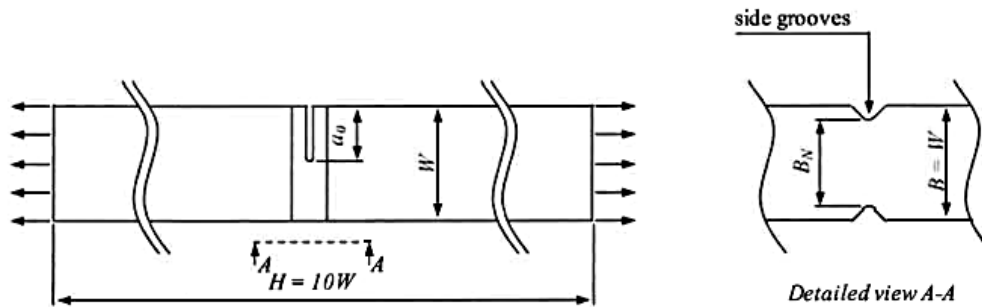


Figure 1: Schematic representation of SENT specimen with indication of main geometrical parameters [8]

As a particular consequence of the free surface boundary condition explained in section 2, the theoretical slip line solution of a homogeneous SENT specimen consists of straight lines originating from the crack tip and having an angle of 45° with the surface. Nevertheless more complicated slip line patterns are experimentally observed for SENT specimens sampling heterogeneous welds [11].

4 EXPERIMENTAL

4.1 Material

The specimens tested do not contain a weld. The SENT test specimens are API-5L X70 [12] high strength pipeline steel. They are extracted from the same plate, adjacent to each other. From standard tensile testing (full thickness prismatic specimens, oriented in the same direction as the SENT specimens), the yield stress (characterized as 0.2% proof stress) amounts to 580 MPa and the ultimate tensile strength to 760 MPa ($Y/T = 0.76$).

4.2 Test layout

Two SENT tests were carried out on a 150 kN hydraulic universal test rig. A speckle pattern for digital image correlation (DIC) was applied for post-processing and reconstruction of the slip line pattern (DIC is elaborated in the next paragraph). Using DIC as post-processing enables to track the path of maximal strains, i.e. the slip lines.

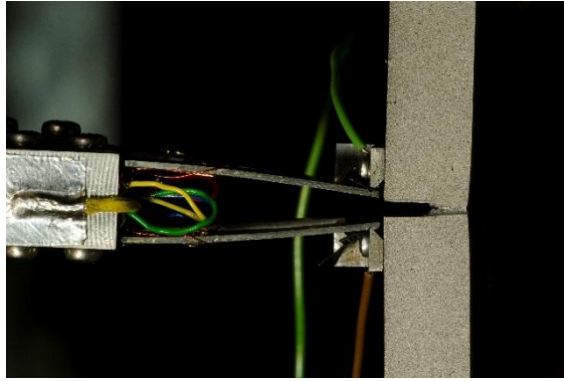


Figure 2: Test layout of digital image correlation with SENT

The specimens have a square cross section, with B and W equal to 12.5 mm. The initial notch has a relative depth a_0/W equal to 0.3 for both specimens. The initial notch tip radius of $75 \mu\text{m}$ was obtained by milling. While one specimen was plane sided, the side grooves in the other specimen gave rise to a total reduction of 10% of the specimen width (5% at either side). This can be considered the only difference of any significance between both specimens.

4.3 Digital Image Correlation

Digital image correlation (DIC) is an optical technique that allows for full field deformation and strain measurements. The 3D DIC technique uses two synchronized cameras which take pictures at predefined time steps. The specimen is painted white, after which a random black speckle pattern is sprayed on top of it. The optimal speckle size depends on the window covered by the cameras, a size of 3 by 3 pixels being advised for the sake of strain accuracy. The displacement of the speckles in the x , y and z direction are tracked by the DIC software by correlating the photos made. By derivation, 3D displacements and 2D strains in the plane of the specimen are obtained. The DIC software allows to easily map these strains and displacements [6], [13]–[15].

4.4 Post-processing

In Matlab® a code has been written to extract the slip lines from the DIC output files. In DIC software, data are extracted according to a grid pattern shown in figure 3. The grid is deforming along with the specimen, so each grid point is followed through the test. The grid extraction and evaluation is conducted for each picture taken by the DIC software. As such, slip line evolutions during the test can be observed. The slip lines are obtained by connecting positions of maximum equivalent total strain (Eq. 9, where ε_1 and ε_2 represent in-plane principal strains) out of each data array of points corresponding with the through-thickness direction in the specimen (horizontal array of points in figure 3).

$$\varepsilon_{eq} = \frac{2}{\sqrt{3}} \sqrt{(\varepsilon_1^2 + \varepsilon_2^2 + \varepsilon_1 \varepsilon_2)} \quad (9)$$

So the total equivalent strains are taken as a measure for the shear stresses linked with slip lines, as the shear stress is dominating the total stress in the slip line region. The angles α_t and α_b represent the slip line angle for the upper ('top') and lower ('bottom') slip line respectively. These angles are obtained from a linear regression of each slip line trajectory.

Evaluations have been done for various grid mesh resolutions, varying from 30 by 120 (60 at either side of the notch) to 50 by 200 (100 at either side of the notch). A grid resolution of 50 by 200 has been selected as its corresponding calculation time was acceptable, and the resulting slip line resolution was considered sufficiently high. Concretely, given the specimen thickness of 12.5 mm, the chosen grid results in a resolution of 0.25 mm on slip line position in both the longitudinal and the through-thickness direction.

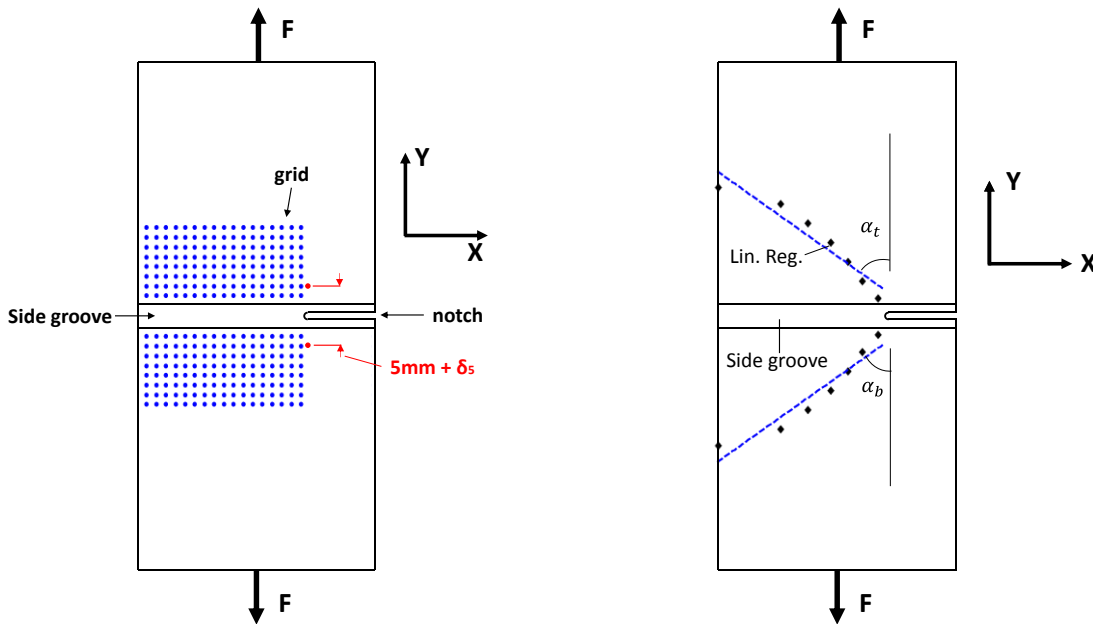


Figure 3: Definition grid pattern, δ_5 and slip line angles

5 NUMERICAL

The finite element software ABAQUS[®] has been used to simulate the performed SENT tests. A Python[™] script, used to generate and analyze SENT tests in ABAQUS[®] and developed by Verstraete [5], has been adopted. Post-processing has been extended to enable the extraction of data along a grid pattern as in figure 3. Similar to the experimental post-processing procedure, evaluation lines have been defined in the through thickness direction. At each intersection with the finite element mesh, nodal displacement and strain are evaluated. Slip lines are based on deformed coordinates and result from a connection of points of maximum plastic equivalent strain over each of the evaluation lines. Assuming proportional plasticity (which is the case for SENT testing), this can be considered as the plastic component of von Mises strain as obtained through DIC in experimental SENT testing. This slight deviation between experimental and numerical analyses is acceptable, given the extent of plasticity expected.

The slip line pattern is extracted at different stages of the simulation (i.e. different levels of crack driving force). Here, too, the slip line angles of figure 3 are obtained from linear regression analysis.

6 RESULTS AND DISCUSSION

In order to compare the experimental and numerical results with the theoretical value of 45°, the slip line angle of both upper and lower slip line are plotted with respect to the crack tip opening. For the experimental results, the δ_5 definition is applied, i.e. tracking the displacement of two points at both sides of the original crack tip initially 5 mm apart. The numerical simulation output provides the crack tip opening displacement according to Rice's 90 degree intercept definition (CTOD₉₀). Both have been shown to produce similar measurements of CTOD in [9].

6.1 Evolution of the slip line angle

Figure 4 plots the slip line angles for the specimen without side grooves (left) and with side grooves (right). The top and bottom slip line refer to the experimental results while only one angle is drawn for the simulations. Indeed, as the specimen is symmetric and has homogeneous material properties the angles of simulated top and bottom slip lines are equal. Similarly, the slip line angles of top and bottom experimental slip lines are close. Furthermore, the angle tends to increase somewhat for CTOD values above 1.5 mm. This is related to the specimen deformation, more specifically to the bending of the specimen around its uncracked ligament. Overall, simulations and experiments agree fairly well.

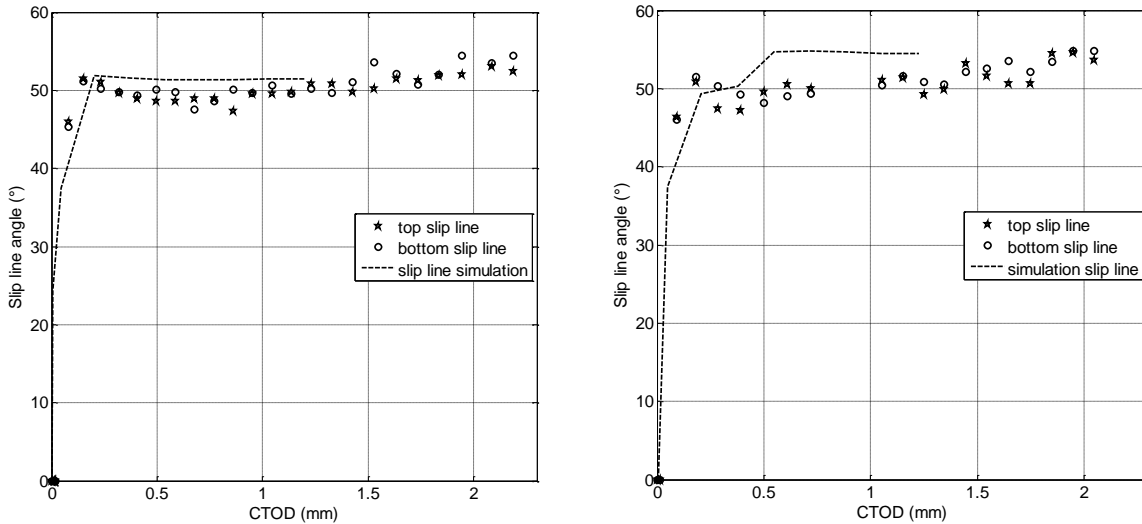


Figure 4: Slip line angles for the specimen without side grooves (left) and with side grooves (right)

In figure 4, the slip line angle varies around 50°. From theory, it is expected that this angle would be 45° in homogeneous material. This 5° difference is related to the deviation of the slip line from its linear trend when approaching the surface (figure 6). If only the intuitively linear portion (which comprises most of the slip line) would be considered, the angle does vary around its theoretical value of 45°, as shown in figure 5. Again, slip line angle is observed to increase upon the application of higher CTOD values.

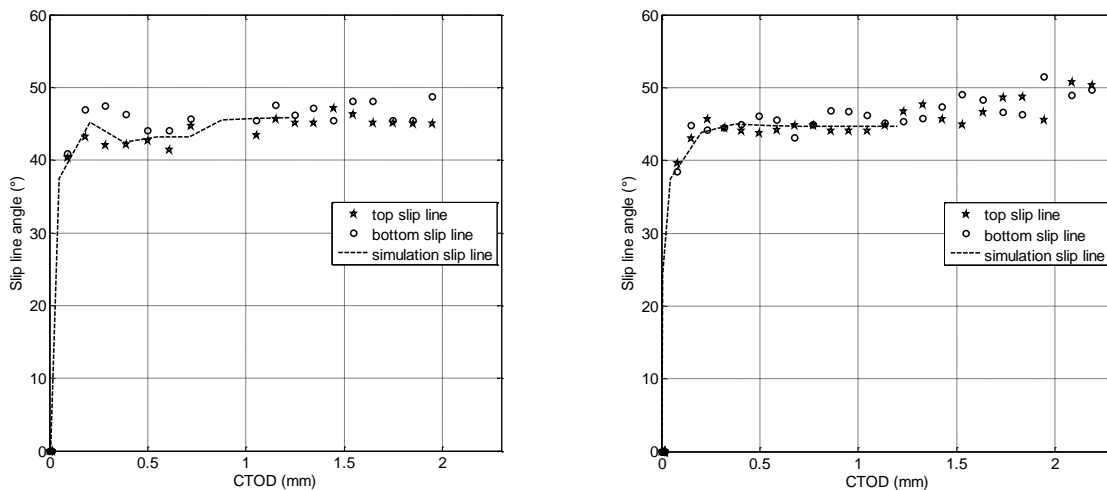


Figure 5: Slip line angles for the linear trend for the specimen without side grooves (left) and with side grooves (right)

The experiments do not seem to indicate that side grooves have a significant effect on the slip line angle as left and right graphs in figures 4 and 5 are similar. In figure 4, the slip line angle for the simulations increases with around 3° when the specimen is side grooved, from around 51° for the non-side grooved specimen to around 54° for the side grooved specimen. Nonetheless, if only the linear trend is analyzed (figure 5), the angle remains around 45° for both specimens. Also, the slip line angle remains constant during most of the simulation. This constant angle is acknowledged when observing the graphs in figure 6. They show in blue the slip lines at the start of the simulation and in red those at the end of the simulation.

Their respective linear regression lines are colored green. The applied displacement for the simulations was 0.9% of the specimen length between the grips, while this value was around 2% for the experiments (more than twice as high). The specimen deformation is consequently much less in the simulations and, therefore, the angle increase is not observed for the simulations.

Finally, the difference in angle for the side grooved and non-side grooved simulations in figure 4 can be explained when studying the propagation behaviour of the plastic region. With side grooves, this region firstly grows along the groove before the slip lines are developed. If the specimen is not grooved, the plastic region does not grow in the notched ligament but rather along with the slip lines. Through its higher strains in the side groove, the groove will operate as a hinge for a profounder bending of the specimen around the uncracked ligament. This results in higher slip line angles.

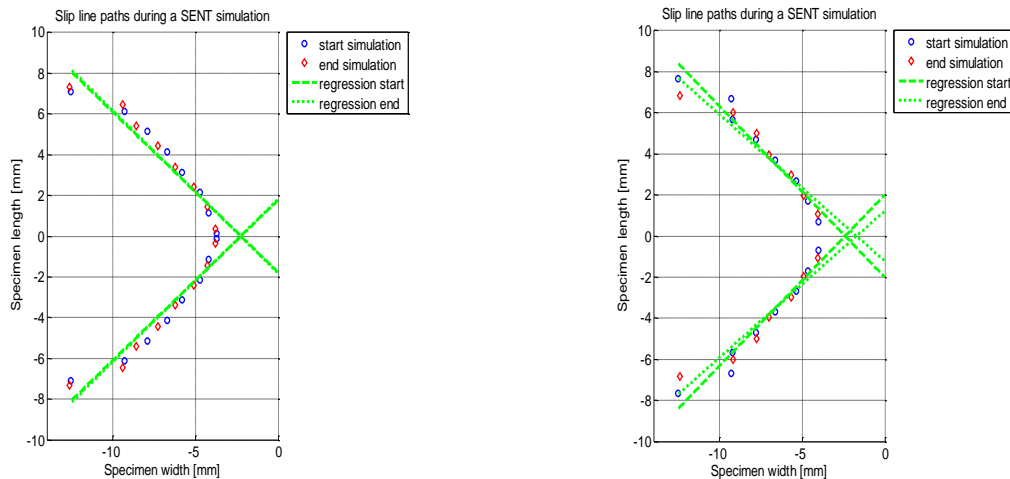


Figure 6: Simulation slip lines without side grooves (left) and with side grooves (right)

7 CONCLUSIONS

From plasticity theory, slip lines should develop under an angle of 45° for a SENT test sampling plain base material (i.e., not containing a weld). At Soete Laboratory, slip line evolutions in SENT specimens have been obtained and analysed in two ways: the experimental way, in which the slip line evolution is extracted with DIC and post-processed in Matlab[®], and the numerical way, using commercial finite element software. The verification of both approaches with theory has been successful. The slip lines angles, determined by linear regression, attain a value of 45° in the specimen for these tests, but the angle increases when approaching the surface. When applying side grooves, the slip line angle slightly increases as the grooved section will concentrate higher plastic strains. Consequently, it will act as a plastic hinge promoting bending of the specimen around its uncracked ligament.

8 ACKNOWLEDGEMENTS

The author would like to acknowledge the support of Soete Laboratory's technical staff.

9 REFERENCES

- [1] G. Wilkowski, D. Rudland, D. J. Shim, and F. W. Brust, "Advanced integration of multi-scale mechanics and welding process simulation in weld integrity assessment", Technical report 14040-1 2008.
- [2] Hill R., *The Mathematical Theory of Plasticity*, Oxford University Press, ISBN 0198503679, 1950.
- [3] Gao H., "Boundary value problems in plasticity: Slip line theory", *Advanced Mechanics of Solids*, Brown University, 2006.
- [4] Johnson H.H., "Calibrating the Electric Potential Method for Studying Slow Crack Growth", *Materials Research Standards*, Vol.4, pp. 442–445, 1965.

- [5] Verstraete M., "Experimental-Numerical Evaluation of Ductile Tearing Resistance and Tensile Strain Capacity of Biaxially Loaded Pipelines", Ph.D. thesis, Ghent University, 2014.
- [6] Hertelé S., Verstraete M., Van Minnebruggen K., Denys R., and De Waele W., "Applications of digital image correlation in girth weld testing," *6th International Pipeline Technology Conference*, Ostend, Belgium, 2013.
- [7] Verstraete M., Hertelé S., Denys R., Van Minnebruggen K., and De Waele W., "Evaluation and interpretation of ductile crack extension in SENT specimens using unloading compliance technique", *Engineering Fracture Mechanics*, vol. 115, pp. 190–203, January 2014.
- [8] Verstraete M., Hertelé S., Van Minnebruggen K., Denys R., and De Waele W., "UGent guidelines for SENT testing", *6th International Pipeline Technology Conference*, Ostend, Belgium, October 2013.
- [9] Verstraete M., Denys R., Van Minnebruggen K., Hertelé S., and De Waele W., "Determination of CTOD resistance curves in side-grooved Single-Edge Notched Tensile specimens using full field deformation measurements", *Engineering Fracture Mechanics*, no. 110, pp. 12–22, 2013.
- [10] Zerbst U., Ainsworth R.A., Beier H.T., Pisarski H., Zhang Z.L., Nikbin K., Nitschke-Pagel T., Münstermann S., Kucharczyk P., and Klingbeil D., "Review on fracture and crack propagation in weldments – A fracture mechanics perspective", *Engineering Fracture Mechanics*, no. 132, pp. 200–276, June 2014.
- [11] Hertelé S., De Waele W., Verstraete M., Denys R., and O'Dowd N., "J-integral analysis of heterogeneous mismatched girth welds in clamped single-edge notched tension specimens", *International Journal of Pressure Vessels and Piping*, vol. 119, pp. 95–107, July 2014.
- [12] American Petroleum Institute, "API 5L, Specification for Line Pipe," no. 45, 2012.
- [13] K. Van Minnebruggen and D. Van Puyvelde, "Experimentele evaluatie van plastische vervormingen en scheurgroei in gelaste constructies", MSc dissertation, Soete Laboratory, Ghent University, 2011.
- [14] Verstraete M., Denys R., Van Minnebruggen K., Hertelé S., and De Waele W., "Determination of CTOD resistance curves in side-grooved Single-Edge Notched Tensile specimens using full field deformation measurements", *Engineering Fracture Mechanics*, vol. 110, pp. 12–22, September 2013
- [15] Sutton M.A., Orteu J.J., and Schreier H.W., *Image Correlation for Shape, Motion and Deformation Measurements*. Springer US, ISBN 9780387787466, 2009.